Amelioration of mesoporous surface by varying concentration of ZnO to eliminate Methylene blue: characterization, kinetics modules and thermal parameter

Lalia Foud[1], Abeer Emam[1], Asmaa Kamal Eldeen[1*], Marwa Ibrahim[2] and Mona Seif[2]
1- Department of Chemistry, Faculty of Science, Al-Azhar Univ. (Girl branch), Cairo, Egypt
2- Department of Chemistry, Faculty of Education, Ain Shams Univ., Roxy, Cairo, Egypt
*Asmaaelzayat146@gmail.com

ABSTRACT

Adsorption assessment of ZnO-SiO_2 (ZSnc) by UV/Vis spectro-photometery was used to monitor the removal of the cationic dye (MB)from waste waters. Silica nanoparticles with a high adsorption capacitywere prepared by sol-gel method. SiO_2 modification was done bydissolving various ratios of zinc oxides at 10%, 30%, 50%, 70% and 90%.With a view to explain the adsorptive characteristics, they were portrayed by XRD, TEM, EDX, SEM, N_2adsorption/desorption isotherms techniques and FT-IR.

The results showed that anamorphous shape and porous structure were obtained by the sol-gel method. The calcination time of nanomaterial and concentration of MB have a significant effect on the adsorption efficiency. The equilibrium data were evaluated using the Langmuir and Freundlich isotherms in order to determine the best adjustment to the experimental data. Langmuir model has been the most appropriate for fitting the experimental data. Additionally, the adsorption kinetics is best described by the pseudo-second order model at a different concentration. Values demonstrated that the adsorption process is exothermic, spontaneous, and favorable. The results elucidated the potential for a new utilize of mesostructured nanomaterial as an active adsorbent.

Keywords: ZnO-SiO_2=ZSnc; Cationic dye; Adsorption; Kinetics.

INTRODUCTION

There are numerous procedures by which wastewater dye can be treated. Among them, adsorption is exceedingly used for its maturity and simplicity. Adsorption is manifested in lots of natural systems,chemical, physical, biological, and industrial applications[1,2].Porous materials are known for a long time and used fordifferent purposes, such as filtration, liquid adsorption. During research and evolution of new porous systems,a better control of pore size, a decrease of pore diameter and a well-organized structure are essential to increase base properties. Sol–gel is one of the leading chemical routes which present a simple way of preparing nanosize with required features. Solution synthesis methods of a mixed oxide including the hydrolysis of metal alkoxides or simple inorganic salts have become of importance in the growth of metal oxides like SiO_2 and ZnO[3,4].The most practical and effective solution of the aggregation problem in a colloid process is an encapsulation of nanoparticles in chemically inert material[5].One of theinteresting solutions to solve thisproblem consists of metal oxide in SiO_2. Different chemical manners were previously investigated for the generation of ZnO nanostructure within SiO_2[3,6]. Particle size of ZnO is stable with aging after being included into SiO_2, as the particles are trapped in the solid silica[7].ZnO as well is predicted toplay an important role in its applications due to control over the physical and chemical properties of material[8,9]and the growth of crystals with a specific size and shape[10,11,12].

Lalia Foud *et al.*

The present study deals with silica-coating ZnO nanoparticles and characterized by several techniques.Effects of some operational parameters as a nanoadsorbent loading and initial MB concentration on the adsorptionefficiency were discussed. The adsorption isotherm technique was used to verify the affinity. Isotherm models have been used. It is expected to play a leading role as an effective adsorbent compared to the purification processes and economical ways.

EXPERIMENTAL METHODS

1. Preparation mesoporous of ZSnc

ZSnc nanoparticles were prepared by a sol-gel method. 2 ml Tetraethyl orthosilicate (TEOS) was mixed with 23.5 ml methyl alcohol (CH_3OH), 14.5 ml deionized water and nitric acid 0.08 ml (HNO_3) under vigorous stirring for 1 hr. After, an aqueous solution of $Zn(Ac_3)_2.6H_2O$ with different wt., ratio concentration(0,10,30,50,70and 90%) was added to the above solution under vigorous stirring for 60 min. The reaction was performed at room temperature. The prepared gel was left for 24 hr. Eventually, the obtained gel was dried in oven at $80^{\circ}C$,followed by calcination at $550^{\circ}C$ for 2hr in the air. Furthermore, the effects of different calcinations time were studied for sample 50% ZSnc at (1-3) hrs. All chemicals used in this work are of reagent- grade quality.

2. Characteristics of devices used

Powder X-ray diffraction (XRD) study was carried out using Shimadzu XRD-6000 as with Cu radiation λ=1.54056 Å was used with a scan rate of 4° in 2θ/min. Crystallite size of nanoparticles were calculated using the Schererequation[13]. The morphology of nano-particles is measured using transmission electron microscope (TEM) Hitachi 7500. The SEM (The Scanning Electron Microscope) Model Quanta 250 FEG (Field Emission Gun) connected with EDX Unit (Energy Dispersive X-ray Analyses), with speeding up voltage 30 K.V., magnification14x up to 1000000 and resolution for Gun.1n). The surface properties of nanomaterials were determined by Quanta chromes Instruments, NOVA Touch LX4 (USA). (FT-IR) Fourier transform infrared spectroscopy was recorded on Nicollet IR 6700 spectrometer USA using KBr pellets. UV−visible spectroscopy (UV−vis/DR) was fulfilled on JASCO V-550 spectrophotometer (Japan) supported with an integrating sphere accessory.

3. Adsorption study

The activity of the adsorbents was examined for the adsorption of a cationic dye such as methylene blue (MB). This was performed in batches consisting of MB solution at diverse concentrations (2.5–7.5x 10^{-5}mol/l). The solution was stirred at room temperature and pH=7 to uniformly disperse the adsorbent with a dosage 0.1 g. At various time intervals, the solutions separate using a centrifuge at 4500 rpm for 5 min. The residual concentration of MB was analyzed by UV−Vis spectrophotometer. The adsorption band of MB was taken at a maximum wavelength (λ_{max}= 664) nm and adsorption uptake.

RESULTS AND DISCUSSION
1. Materials Characterization
1.1. XRD

Figure (1) shows the XRD pattern of 50%nanocomposite samples ZSnc with different calcination time (1-3)hrs, at $550^{o}C$.All 50% ZSnc are amorphous structure and the absences of peaks corresponding to ZnO are revealed in XRD patterns. ZnO diffraction peak was scattered from the SiO_2 diffraction with very low intensity. XRD of 90% ZSnc shows hexagonal wurtzite diffraction peaks at 2θ =31.71^{o}, 34.48^{o}, 36.23^{o}, 47.53^{o}, 56.47^{o}, 62.78^{o}, and

Amelioration of mesoporous surface by varying concentration of ZnO to eliminate Methylene blue**: characterization, kinetics modules and thermal parameter**

67.92^oin Fig1. These arerelated to the (100), (002), (101), (102), (110), (103) and (112) planes of the ZnO[14]. The Scherer formula is used to calculate crystalline size and it is found 20.5 nm
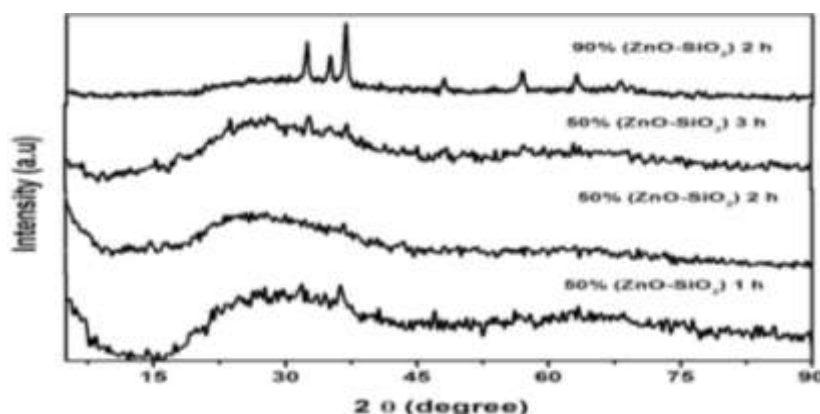
Fig .1: XRD Patters of 50% ZSnc at different calcinations time and 90% ZSnc.

1.2. TEM & SEM

In order to inspect the morphology of the nanoparticles TEM and SEM were measured.
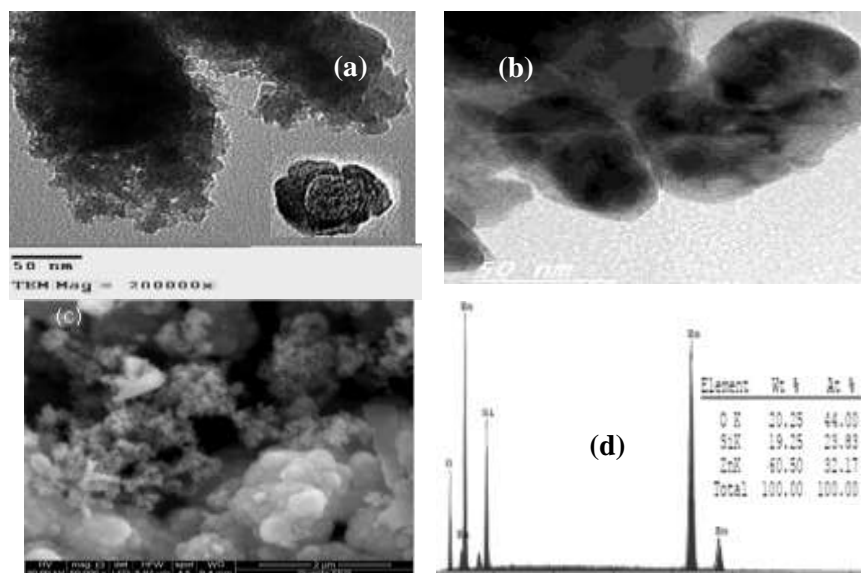
Fig 2: TEM image of 50% ZSnc (a) and 90% ZSnc TEM (b), SEM (c), EDS (d).

Figure (2 a,b) showed the TEM morphology of 50%ZSnc and 90% ZSnc, respectively. 50% ZSnc shows high aggregation of particles as appeared in Figure(2a). While, 90% ZSnchas a low aggregation hybrid morphologies (spherical, nano sheets) with mean diameter 18 nm and this data is rhythmic with XRD measurements. The SEM is used in order to study the surface morphology of 90% ZSnc and the results show the assemblage particles as in Figure (2c). The EDX analysis was also performed to underline the composition of the 90% ZSnc and it is proved the presence of Zn, Si and oxygen elements in Figure (2d).

1.3. Surface area measurements

The nitrogen adsorption-desorption isotherms are given in Figure (3a).Pure silica is the type II which is typical of either nonporous or mixed pore system according to IUPAC. Yet,

Lalia Foud *et al.*

50% and 90% ZSnc are exhibiting type IV isotherm, which is the typical adsorption profile for mesostructure[15]. Figure (3b). Elaborates the pore size distribution obtained from the desorption branch of the isotherms. The textural properties, including specific surface area (S_{BET}), monolayer volume (V_m), total pore volume (V_P) and mean pore diameter derived from the N_2 adsorption-desorption isotherms and pore size distributions of all binary oxides are summarized in Table (1). Data indicates that the specific surface areas and (V_m) of ZSnc which are reduced by the increase in the content of ZnO as manifested by XRD and TEM results. Pore volume results also go along with this observation[16].The average values of pore radius (ŕ) appear similar to all samples and never more than 2.5 nm, indicating that very small cavities have size near the boundary of mesopores which responsible for most porosity in samples. The pore size distribution presented in Fig 3a display that pure SiO_2 sample possess has a narrow distribution in the microporous region in addition to small amount of mesopores with an average pore diameter of 1.4 and 3.7 nm, respectively. However, the pore size distribution of ZSnc with different ZnO content show a relatively narrow distribution in mesoporous range with an average pore diameter of 2.1 and 2.6 nm. So, the ZnO loading on SiO_2 significantly changes the average micropores diameter of the SiO_2 to mesoporous with increasing the content of ZnO.

Table1. Surface area and pore size distribution analysis of nano particles.

Samples	S_{BET} (m²/g)	V_m (cm³/g)	V_P (cm³/g)	ŕ (nm)	Mean pore diameter (nm)
SiO_2	396.18	0.11	0.24	1.2	2.5
50%	188.15	0.05	0.24	2.5	2.1
90%	151.98	0.04	0.19	2.5	2.6
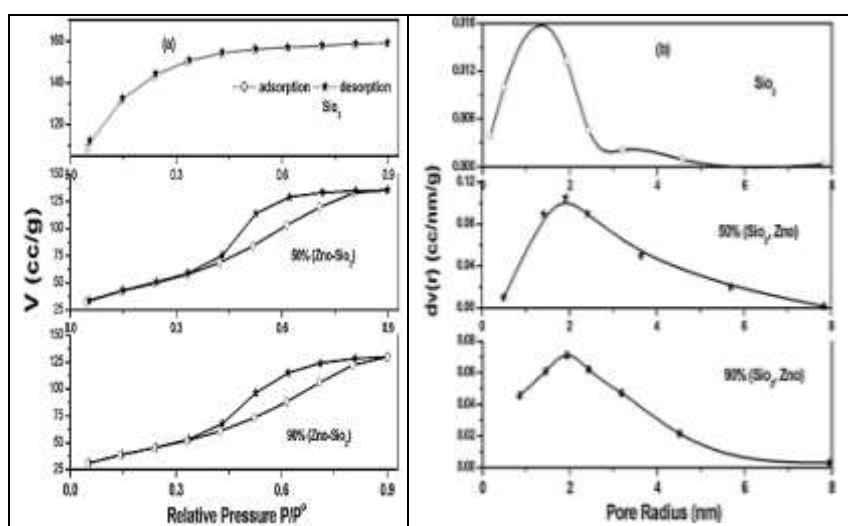
Fig 3: (a) Nitrogen adsorption–desorption isotherms of SiO_2, 50% ZSnc and 90% ZSnc, (b) Pore size distribution of the SiO_2, 50% ZSnc and 90% ZSnc

Amelioration of mesoporous surface by varying concentration of ZnO to eliminate Methylene blue**:**
characterization, kinetics modules and thermal parameter

1.4 FT-IR

FT-IRspectra of unmodified and modified silica are stated in Fig 4.The high wavelength spectral range, a broadband around 3446 cm^{-1}is assigned to stretching vibration of distinct surface hydroxyl groups (free or bounded).The band at 1635cm^{-1}is related tomolecular water[17]. In addition, the peaks at 2854 and 2925 cm^{-1} corresponded to the stretching vibrations of H-O-H bond[18].
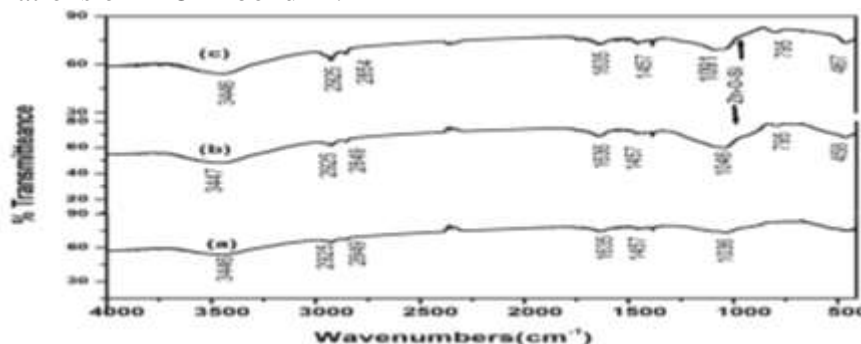
Fig.4: FTIR spectra of (a) SiO$_2$; (b) 50% ZSnc and (c) 90% ZSnc.

A broad band at 1457 cm^{-1}match the Si−O stretching vibrations as well as the Si−O−Si deformation vibrations[19].The absorption peak at about795 and 1090 cm^{-1} is indexed to the symmetric stretching of the Si–O–Si group[20,21].Whereas the peak of Zn-O-Si appears at 910 cm^{-1}associated with increasing ZnO[22]. Particularly significant features are the absorption bands at 466 and 458 cm^{-1}.which could be assigned to the stretching vibration of Zn-O bond[24] as in Figure (4b,c), respectively. These results from FTIR are compatible with XRD.

3.2. Adsorption study
3.2.1. Kinetics studies

Adsorption kinetics is essential for understanding the adsorbate uptake rate and the mechanism of the process.The elimination of MB from the solution by adsorption onto different adsorbents obtained by batch contact time studies for a dye concentration of 5x10^{-5}mol/l was presented in Figure(5a).It was obvious that the 50% ZSnc removes dye efficiently. This is due to it has a large specific surface area and smaller pore radius as well as exceptional mesoporous structures. Also, it can be deduced that the equilibrium time relies on adsorbent surface features and adsorbate, while it does not rely on adsorbent size[23].The high dye removal efficiency was observed in case of 50% ZSnc with 20 min of reaction time. The calcination time effect on the dye removal and two hours of calcination is the preferable time to the decolorization of dye in Fig 5b.Also, indicated that the dye uptake increased with time and, at some point in time,reached a constant value where no more dye was removed from the solution. The equilibrium time was found to be (60 -150) min for otheradsorbents (10%, 30%, 70% and 90%) of the samples. However, the speedy adsorption noticed during the first 5min is probably reasons for the abundant availability of efficient sites on the surface of the adsorbent.

Lalia Foud *et al.*
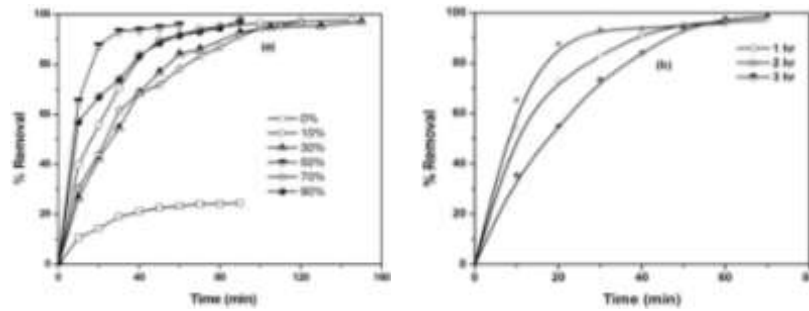
Fig. 5: (a) MB removal % as a function of time at different concentration ZSnc adsorpitily, and (b) different calcinations time (1-3 hrs) at 50%ZSnc.

The experimental data from thisstudy were fitted to three traditional kinetic models, as pseudo-firstorder[24], pseudo-secondorder[25] and intra-particle diffusion model[26]. The values of the parameters, correlation coefficient obtained from these three kinetic models are all listed in Table (2).Pseudo-first order equation:

$$In\ (q_e - q_t) = In\ (q_e) - k_1 t \qquad (1)$$

Where q_e and q_t (mg/g) are the amounts of MB adsorbed at equilibrium and at time t(min), respectively, and $k_1(min^{-1})$ is the adsorption rate constant.

As in Figure (6a),based on Table (2), the linear regression coefficients obtained from the pseudo firstorder kinetic model were found to be low. Furthermore; there were remarkable distinctions between the calculated and experimental q_e values, pointing out that the first order model does not reproduce adsorption kinetics of MB on catalysis.Pseudo-second order equation:

$$\frac{t}{q_t} = \frac{1}{k_2 q_e^2} + \frac{t}{q_e} \qquad (2)$$

Where k_2 (g/mg.min) is the rate constant of second orderequation.Fig.(6b) and Table (2) were evidence stellar linearity, the results showthat the pseudo secondorder kinetic model accords with experimental data perfect with linear regression coefficients of $(R^2 > 0.999)$at all different concentrations of adsorbents. The calculated q_e values for the pseudo-secondorder kinetic model demonstrate good harmony with the experimental q_e values, as in Figure (6b).

The intra-particle diffusion model can be described as:

$$q_t = k_{id} t^{\frac{1}{2}} + C \qquad (3)$$

Where k_i is the intra-particle diffusion rate constant (mg/g.min$^{1/2}$) and C is the intra-particle diffusion constant, commonly the intra-particle diffusion model is used to recognize the mechanism engaged in the adsorption process.In this model suggests that intra-particle diffusion is the rate-controlling step, which is mostly the state for well-mixed solutions. In this model the adsorbed amount q_t should differ linearly in the square root of time. As shown in Figure (6c) and Table (2).Uncovered that the diagram is not linear along the whole time range; yet, it exhibits a bi-linearity, revealing the presence of two successive adsorption phases of mass transport with a low rate[27].It is influential to note the fact that when the first linear diagrams do not pass through the origin, this is indicative of some degree of boundary layer control and further clears that the intra-particle diffusion is not the only rate controlling step, but some other processes may control the rate of adsorption[28].

Amelioration of mesoporous surface by varying concentration of ZnO to eliminate Methylene blue**:**
characterization, kinetics modules and thermal parameter
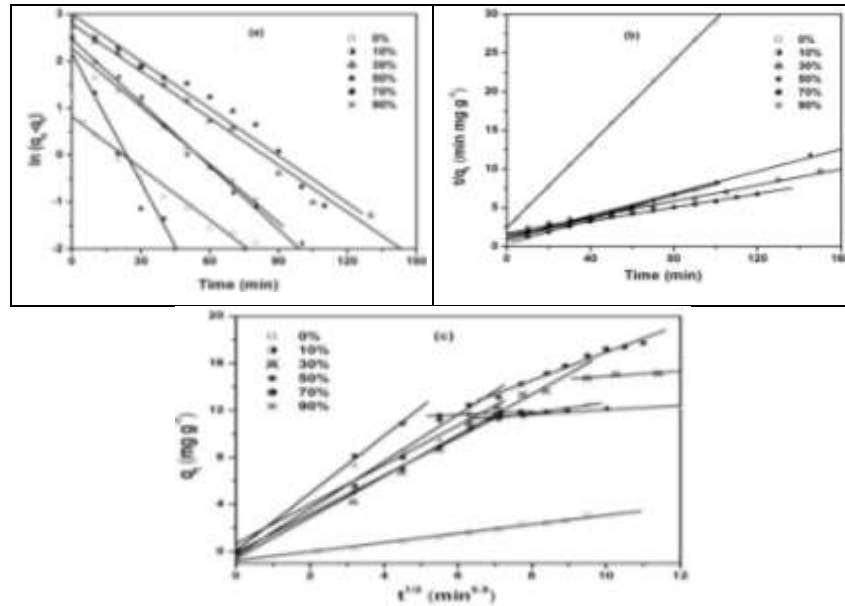
Fig.6: (a) Pseudo-first order kinetics model, (b) Pseudo-second order kinetics model, (c)
Intra-particle diffusion model plot over different adsorbents of ZSnc.

Table2. Kinetic parameters for the adsorption of MB (5x10^{-5}mol/l)on different
concentrations from adsorbents (adsorbent mass10 mg and calcination 550°C).

Different adsorbentsat 2 hours calcination	$q_{e.exp}$ (mg/g)	Pseudo-first-order model $q_{e.cal} K_1 R^2$ (mg/g) (min^{-1})		Pseudo-second-order model $q_{e.cal} K_1 R^2$ (mg/g)(g.mg^{-1}min^{-1})		Intra-Particle-diffusion C $K_{dif} R_1^2$ (mg g^{-1}min^{-1})	
0%	3.5	2.3	0.04 0.96	3.70	0.03 0.99	2.23 0.12 0.95	
10%	12.4	11.8	0.05 0.98	13.9	0.005 0.99	10.1 0.20 0.86	
30%	15.4	16.3	0.03 0.98	19.2	0.002 0.99	12.7 0.22 0.92	
50%	11.9	8.7	0.09 0.96	12.9	0.020 0.99	10.8 0.15 0.96	
70%	17.7	20.1	0.03 0.96	22.7	0.001 0.99	3.82 1.35 0.96	
90%	12.5	9.7	0.04 0.98	13.9	0.006 0.99	0.18 0.45 0.97	
50% 1 hr.	14.1	19.3	0.08 0.96	17.8	0.003 0.98	12.5 0.18 0.99	
50% 3 hr.	14.2	21.1	0.07 0.92	21.3	0.002 0.99	9.70 0.55 0.88	

2.2. Adsorption Isotherms Models

The analysis of the equilibrium adsorption isotherm model is a prerequisite for predicting the adsorption uptake of the adsorbent, which is one of the major parameters needed for designing optimized adsorption system. An available isotherm models, that is, Langmuir and Freundlich models [28] were used for this objective. The linear forms of isotherm models were facilitated and represented in Figure (7) and Table (3) as follows:

2.2.1. Langmuir Isotherm

The Langmuir adsorption isotherm has been successfully applied to various pollutant adsorption operations from aqueous solution.The linear form of the Langmuir model is represented as follows

$$\frac{C_e}{q_e} = \frac{C_e}{Q_0} + \frac{1}{bQ_0}(4)$$

C_e is the liquid-phase concentrations of dye at equilibrium (mg/l), q_e the amount of dye adsorbed at equilibrium (mg/g), Q_0 the maximum monolayer adsorption capacity (mg/g) and b the Langmuir constant (L/mgor L/mol). A linear plot of (C_e/q_e) *vs.*C_e is obtained from the Langmuir model, as shown in Fig. 7a. From the value of b deduced from the Langmuir model, the equilibrium parameter $R_L$was calculated using the following equation

$$R_L = \frac{1}{1+bC_0}(5)$$

Value of R_L indicates the isotherm is inconvenient ($R_L>1$), linear ($R_L=1$), convenient ($0<R_L<1$) or irreversible ($R_L=0$). C_0 is the initial dye concentration. The R_L values for MB adsorption over various concentration catalysis were less than one and greater than zero, showing a favorable adsorption in Table 3and Fig. 7a.The MB adsorption capacity increased in all ZSnc than pure SiO_2 due to the MB on ZnO surfaces was more mobile so that the diffusion of MB on ZSnc was easier than on bare SiO_2 at the initial stage of theadsorption experiments. In addition to, the maximum monolayer adsorption capacity of 50% ZSnc decreases with increasing the rate removed MB at (5×10^{-5}mol/l).This is due to the electrostatic repulsive forces between adsorbent and dye molecules might also take part into resisting the adsorption of MB and lead to lower adsorption ability.

2.2.2. Freundlich Isotherm

The Freundlich isotherm model depicts the adsorption of solutes from a liquid to a solid surface and assumes that different sites with assorted adsorption energies are involved. It gives a clarification of the adsorption equilibrium between an adsorbent in solution and the surface of the adsorbent, using a multi-site adsorption isotherm for heterogeneous surfaces. The Freundlich model can be represented by the linear form as follows:

$$\text{In}q_e = \text{In}k_f + \frac{1}{n}\text{ In }C_e(6)$$

Since C_e is the liquid-phase concentrations of dye at equilibrium (mol/l) and q_e the amount of dye adsorbed at equilibrium (mg/g).The value of n, which is recognized as heterogeneity factor, was used to identify the adsorption whether it is linear n=1,chemical processn <1, and physical process n>1.In this studylinear adsorption process is convenient with the n value 1, however the K_F value, which is an indicator of adsorption capacity, indicated a high MB adsorptive capacity of adsorbent from aqueous solution[29]. The inconsistent arrangement of theheterogeneously adsorbed MB has been shown to reinforce the progression of local multilayers[30]. In general, as the K_F rises the adsorption capacity of the adsorbent increases. Its correlation coefficients ($0.94<R^2<0.99$) are much lower than those for the Langmuir isotherm, suggesting that the Langmuir isotherm model is the preferable model to fit the experimental data.

Amelioration of mesoporous surface by varying concentration of ZnO to eliminate Methylene blue**: characterization, kinetics modules and thermal parameter**
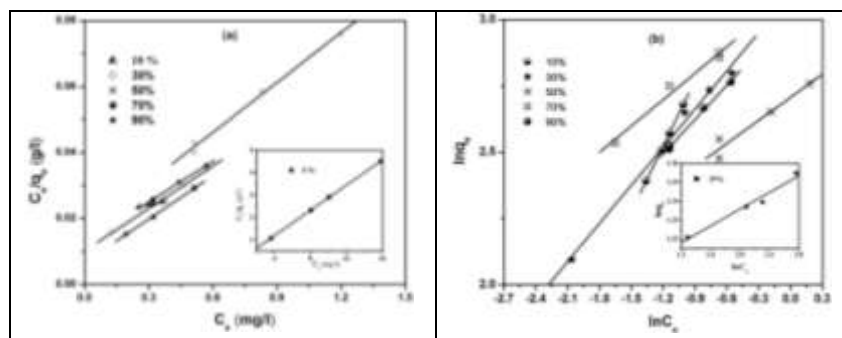
Fig.7: (a) Langmuir isotherm models (b) Freundlich isotherm modelsfor adsorption of MB on different adsorbents of ZSnc.

Table 3. Isotherm models for the adsorption of MB (5×10^{-5}mol/l) on different concentrations from adsorbent (adsorbent mass:10mg at calcination550°C).

Different concentrations adsorbents	Langmuire				Freundlish		
	q_{max} (mg/g)	b (Lg^{-1})	R_L (Lmg^{-1})	R^2	K_f (mg g^{-1})	n	R^2
0%	18.37	0.19	0.21	0.99	3.29	45.3	0.97
10%	69.4	0.73	0.084	0.98	33.44	1.5	0.99
30%	23.32	4.2	0.016	0.99	22.06	2.1	0.99
50%	19.85	3.2	0.02	0.99	15	3.4	0.94
70%	22.67	6.7	0.01	0.99	22.1	3	0.98
90%	24.22	3.28	0.02	0.99	20.35	2.3	0.99

Conclusions

In this study, highly effective adsorbent ZSnc with different content of ZnO for adsorption of cationic dye (methylene blue) has been prepared by sol-gel method. Raising the amount of ZnO affected on the crystallinity, morphology and surface area of SiO_2.Where 50% ZSnc has the highest adsorption rate of removal of dye. In addition to, the experimental results fit well with the pseudo second order model and Langmuir isotherm.

REFERENCES

1-K.Czelej; K. Cwieka and K.J. Kurzydlowski (2016). CO_2 stability on the Ni low-index surfaces: Van der Waals corrected DFT analysis, Catal. Commun. 80: 33-38.

2- K.Czelej; K. Cwieka; J. C. Colmenares and K.J. Kurzydlowski (2016).Insight on the Interaction of Methanol-Selective Oxidation Intermediates with Au- or/and Pd-Containing Monometallic and Bimetallic Core@ShellCatalysts, Langmuir., 32 (30): 7493-7502.

3-Y. Ohya; H. Saiki; Y. Takahashi and J. Mater. (1994). Preparation of transparent, electrically conducting ZnO film from zinc acetate and alkoxide, Sci., 29:4099-4103.

4-W. Stöber; A. Fink and E. Bohn (1968). Controlled growth of monodisperse silica spheres in the micron size range, J.Colloid. Interface.Sci. 26: 62-69.

5- L. Shastri; M.S. Qureshi and M.M. Malik (2013).Photoluminescence Study Of ZnOSiO$_2$ Nanostructures Grown In Silica Matrix Obtained Via Sol Gel Method, J.Phys.Chem.Solids,74(4) : 595-598.

6- M.Abdullah; S. Shibamoto and K. Okuyama (2004).Synthesis of ZnO/SiO$_2$ nanocomposites emitting specific luminescence colors, Opt.Mater.26:95-100.

7- A. Spoiala; I.A. Nedelcu; D. Ficai; A. Ficai and E. Andronescu (2013).Zinc Based Antibacterial Formulations for Cosmetic Applications, J. Nanomater . Biostruct., 8 (3):1235-1242.

8-A. B.Djurišić; X.Chen; Y. H.Leung and A. M. C.Ng (2012). ZnO nanostructures: growth, properties and applications, J. Mater. Chem. 22 : 6526-6535.

9- M. Yoshimura and K. Byrappa (2008).Hydrothermal processing of materials: past, present andfuture,J. Mater. Sci., 43:2085-2103.

10- B. Liu and H.C. Zeng (2003). Hydrothermal synthesis of ZnO nanorods in the diameter regime of 50 nm,J. Am. Chem. Soc., 125(15): 4430-4431.

11-Y. Masuda; N. Kinoshita and K. Koumoto (2007). Morphology control of ZnO crystalline particles in aqueous solution,Acta,53:171-174.

12- O. Singh; M.P. Singh; N. Kohli and R.C.Sens (2012).Effect of pH on the morphology and gas sensing properties of ZnO nanostructures, Actuators, B: Chem.166 :438-443.

13- H.P. Klug and L.E.Alexander (1966).X-ray Diffraction Procedures for Polycrystalline and Amorphous Materials, John Wileyand Sons, New York, pp. 491.

15- M. G. Jeong; E.J. Park; B. Jeong; D.H. Kim and Y.D. Kim (2014).Toluene combustion over NiO nanoparticles on mesoporous SiO$_2$ prepared by atomic layer deposition, J. Chem. Eng. 237: 62-69.

16- F. Rouquerol; J. Rouquerol and K. Sing (1999). Adsorption by Powders and Porous Solids: Principles, Methodology and Application, Academic Press.

17- M. M. Ibrahim (2015). Photocatalytic activity of nanostructured ZnO-ZrO$_2$ binary oxide using fluorometric method, Spectrochim.Acta. A: Mol. Biomol. Spectrosc. 145: 487-492.

18- S. Asal; M. Saif; H. Hafez; S. Mozia; A. Heciak; D. Moszyński and M.S.A. Abdel-Mottaleb (2011).).Photocatalytic generation of useful hydrocarbons and hydrogen from acetic acid in the presence of lanthanide modified TiO$_2$, Int. J. Hydrogen. Energy. 36:6529-6537.

19- G. Korotcenkov; S. Do Han; B. Cho and V. Tolstoy (2009).Structural characterization and phase transformations in metal oxide films synthesized by Successive Ionic Layer Deposition (SILD) method, Appl. Ceram., 3 (1-2):19-28.

20- H.R. Mahmoud; S.A. El-Molla and M. Saif (2013).Improvement of physicochemical properties of Fe$_2$O$_3$/MgO nanomaterials by hydrothermal treatment for dye removal from industrial wastewater, Powder Technol., 249: 225-233.

21-A.M.Ali; A.A.Ismail; R. Najmy; A. Al-Hajry (2014). Preparation and characterization of ZnO–SiO$_2$ thin films as highly efficient photocatalyst, J. Photochem. Photobiol. A: Chem.,275: 37-46.

22-C. T. Kirk (1988).Quantitative analysis of the effect of disorder-induced mode coupling on infrared absorption in silica,Phys. Rev. B.Condens. Matter. 38(2):1255-1273.

23-J. Zhai; X. Tao; Y.Pu; X-FeiZeng; and J. Feng Chen (2010).Core/shell structured ZnO/SiO$_2$ nanoparticles: preparation, characterization and photocatalytic property, Appl. Surf. Sci. 257 (2): 393-397.

Amelioration of mesoporous surface by varying concentration of ZnO to eliminate Methylene blue:
characterization, kinetics modules and thermal parameter

24-B.K. Suyamboo and R.S. Perumal (2012).Thermodynamic and Kinetic Studies on Adsorption of a Basic Dye by Citrullus Lanatus Rind. J. Energy Environ.3, (1): 23-34.

25-Y. Ho and G. McKay (1998).Sorption of dye from aqueous solution by peat, Chem. Eng. J. 70: 115-124.

26- I. Kiran; T. Akar; A.S. Özcan; A. Özcan and S. Tunali (2006). Biosorption kinetics and isotherm studies of Acid Red 57 by dried Cephalosporium aphidicola cells from aqueous solutions, Biochem. Eng .J., 31(3):197-203.

27- E. R. García; R. L. Medina; M. M. Lozano; I. H. Pérez; M. J. Valero and A. M. M. Franco (2014).Adsorption of Azo-Dye Orange II from Aqueous Solutions Using a Metal- Organic Framework Material: Iron- Benzene tricarboxylate, Mater., 7 (12):8037-8057.

28-I. Langmuir (1916).The Constitution and Fundamental Properties of Solids and Liquids. Part I. Solids, J. Am. Chem. Soc.,38 : 2221-2295.

29- H. M. F. Freundlich (1906).Over the adsorption in solution, J. Phys. Chem., 57:1100-1107.

30- W.D. Harkins and E.J. Jura (1944).Surfaces of Solids. XIII. A Vapor Adsorption Method for the Determination of the Area of a Solid without the Assumption of a Molecular Area, and the Areas Occupied by Nitrogen and Other Molecules on the Surface of a Solid, J. Chem. Phys. 12 (3) : 112.

31- M.J. Temkin and V. Pyzhev (1940).Application of temkin adsorption isotherm, Acta Physiol.Chem USSR. 12: 271.

تحسين السطح المسامي من خلال تركيزات مختلفه من اكسيد الزنك لازاله صبغ ازرق الميثيلين : عن طريق وصف ومقاييس الحركيه والحراريه

ليلى فؤاد محمد اسماعيل[1]، عبيرأحمد امام[1]، أسماء كمال الدين محمد الزيات[1*] ، مروه محمد ابراهيم[2]، منى مصطفى علي سيف[2]

1- كليه العلوم بنات جامعة الازهر.

2 –كليه التربيه- جامعة عين شمس

3 **Lalia Foud[1], Abeer Emam[1], Asmaa Kamal Eldeen[1*], Marwa Ibrahim[2] and Mona Seif[2]**

المستخلص

تم تحضير اكاسيد مختلفه بين ثانى اكسيد السليكا واكسيد الزنك بنسبة (10 ٪ ، 30 ٪ ، 50 ٪ ، 70 ٪ و 90 ٪). لتحسين الشكل البلوري من المركب النانو بواسطه طريقه السول جل . ومن خلال قياسات مختلفه من XRD، TEM ، EDX، SEM،N2 و FT IR. تبين ان المركب له خصائص مورفولوجيه وذات بنيه مساميه من خلال طريقه سول جل. وبناء علي ذلك تم تطبيق الامتزاز علي النسب المختلفه من الاكاسيد وتبين ان وقت تكليس المواد النانوية وتركيز صبغ ازرق المثيلين له تأثيركبير على كفاءة الامتزاز. تم تقييم بيانات التوازن باستخدام قوانين لانجميير وفرندش من أجل تحديد أفضل تعديل للبيانات التجريبية. كان نموذج لانجمير هو الأنسب للبيانات التجريبية. عن طريق استخدام UV Vis/ الطيف الضوئي لقياس التغيرات في صبغة الموجبة (ازرق المثيلين) في تركيزات عدة بالإضافة إلى ذلك ، يتم وصف أفضل السلوك الحركي للامتزازمن خلال نموذج الدرجه الثانيه بتركيزات مختلفه من الصبغ الموضح . وأظهرت القيم أن عملية الامتزاز طاردة للحرارة ومتاحه. كذلك توضح النتائج إمكانية استخدام جديد للمواد النانوية بطريقه السول جل.